

$p < 0.05$ ,  $n=3$ ) and LIV induced  $\beta$ catenin-Nsk association was inhibited in siSUN treated MSCs ( $p < 0.05$ ,  $n=3$ ). **e**) Similarly, siSUN decreased both basal Nsk-bound  $\beta$ catenin to 70% ( $p < 0.05$ ,  $n=3$ ) and inhibited the strain induced  $\beta$ catenin-Nsk association ( $p < 0.05$ ,  $n=3$ ). **f**) Nesprin-2 was immunoprecipitated immediately following LIV and probed against  $\beta$ catenin. LIV decreased Nesprin-2-  $\beta$ catenin association 50% ( $p < 0.001$ ,  $n=4$ ). Please see Fig.S4 for a more detailed blot. Group comparisons were made using unpaired T-test (Figure 4f) and One-way ANOVA followed by a Newman-Keuls post-hoc test (Fig.4a-e). \*  $p < 0.05$ , \*\*  $p < 0.01$ , \*\*\*  $p < 0.001$ , against control and each other.

#### APPENDIX: Supplementary Figure Legends & Tables and Methods

##### Supplementary Figure Legends

**Figure S1. Co-depletion of LINC elements Sun-1 and Sun-2 displaces both Nesprin-2 and  $\beta$ catenin from nuclear envelope** **a**) Immunoprecipitation of Nesprin-2 showed associations between  $\beta$ catenin and Emerin. **b**) Representative images of siCtrl and siSUN treated cells showing Nesprin-2 (red) and  $\beta$ catenin (green) distribution. In siCtrl treated cells, colocalization between Nesprin-2 and  $\beta$ catenin (represented as yellow line) remains intranuclear while in siSUN treated cells colocalization was shifted into perinuclear area and remains outside of the nuclear boundary (DAPI, blue line). Representative images of **c**) siCtrl and siSUN treated cells indicating the intracellular localization of Nesprin-2 (red) and  $\beta$ catenin (green) in relation to the nucleus (blue). White arrows indicate the perinuclear distribution of Nesprin-2 and  $\beta$ catenin in siSUN treated cells.

**Figure S2. Nuclear  $\beta$ catenin accumulation but not  $\beta$ catenin-nucleoskeleton association increase under sustained GSK3  $\beta$  inhibition** **a)** SB415 induced inhibition of GSK3 $\beta$  resulted in a stable increase of soluble nuclear  $\beta$ catenin at 20, 140 and 160 minute time points. **b)** SB415 induced inhibition of GSK3 $\beta$  resulted in an increased  $\beta$ catenin-Nsk association as soon as 20 minutes and upon keeping SB415 constraint,  $\beta$ catenin-Nsk association remained elevated at 140 and 160 minute time points but signal intensity was not changed.

**Figure S3. Depletion of Emerin or LaminA/C is not sufficient to inhibit LIV-induced  $\beta$ catenin-nucleoskeleton association** **a)** siRNA against Emerin (siEMD) did not change the basal and LIV-induced  $\beta$ catenin-Nsk association between siCtrl and siEMD MSCs. **b)** Similarly, siRNA against LaminA/C (siLmna) did not inhibit LIV-induced  $\beta$ catenin-Nsk association. LIV was applied at 90 Hz, 0.7g for 20 minutes. Samples were collected immediately after second LIV application.

**Figure S4. LINC elements Sun-1 and Sun-2 are necessary for strain-induced  $\beta$ catenin nuclear entry.** Application of strain results in **a)** Akt activation as well as **b)** GSK3 $\beta$  in both siCtrl and siSUN treated cells suggesting an increased  $\beta$ catenin pool in the cytoplasm (n=3). **c)** Separating soluble nuclear and cytoplasmic fractions 160 min post-strain showed that in siCtrl cells  $\beta$ catenin entered the nucleus while in siSUN cells there was no increase in nuclear  $\beta$ catenin and  $\beta$ catenin in the cytoplasmic fraction was increased. Group comparisons were made using One-way ANOVA followed by a Newman-Keuls post-hoc test (Fig.S4a-b). \* p<0.05, \*\* p<0.01, \*\*\* p<0.001, against control and each other.

**Figure S5. Nesprin-2 Immunoprecipitation.** Supplementary file for Fig.4f displaying full size blots and other control lanes.

**Figure S6. Comparison of LIV and strain induced changes of Lamin A/C and Lamin B1.** Changes in Lamin A/C and Lamin B1 protein amounts were reported as ratio between **a)** control and LIV samples (n=8) and **b)** control and strain samples (n=6). 120 minutes after the first mechanical challenge, no differences between LaminA/C and LaminB1 was detected in response to either LIV or Strain. Group comparisons were made using unpaired T-test (Figure S6a-b).

**Figure S7. Total  $\beta$ catenin levels did not change with LIV.** Whole cell lysates 160min post-LIV were probed via total  $\beta$ catenin (BD, 610154) and  $\beta$ -Tubulin (Santa Cruz, SC-9104)

**Table.S1 :** Cell Culture and Pharmacological Reagents

Cell Culture and Pharmacological Reagents		Final Concentration
IMDM	GIBCO	-
FBS	Atlanta Biologicals	10% v/v
Penicillin/streptomycin	GIBCO	1% v/v
SB415286	Sigma Aldrich	20 $\mu$ M

**Table.S2 :** Antibodies used and their final concentrations for western blots

Antibodies		Final Concentration
Akt (#4685)	Cell Signaling	1/2000
p-Akt Ser473 (#4058L)	Cell Signaling	1/1000
LaminA/C (#4C11)	Cell Signaling	1/1000
p-FAK Tyr397 (#328 3)	Cell Signaling	1/1000
FAK (sc-558)	Santa Cruz Biotechnology	1/500
RhoA (sc-418)	Santa Cruz Biotechnology	1/1000
Emerin (ab40725)	Abcam	1/1000
Nesprin-2 (IQ565).	Immunoquest	1/500
$\beta$ catenin (#610051)	Milipore	1/2000

**Table.S3 :** siRNA sequences

siRNA Sequences -Stealth Select siRNAs (Invitrogen)	
siRNA SUN-1 Control	5'- GAAATCGAAGTACCTCGAGTGATAT -3'
siRNA SUN-1	5'- GAAAGGCTATGAATCCAGAGCTTAT-3'
siRNA SUN-2 Control	5'-CACCAGAGGCTAGAACTCTTACTCA-3'
siRNA SUN-2	5'-CACCAGAGGCTAGAACTCTTACTCA-3'
siRNA Emerin Control	5'-CAACCCUUACUCG-GGUAUCUAGGUG-3'
siRNA Emerin	5'-CAACAUCCCUCAUGGGCCUAUUGUG-3'
siRNA Lamin A/C Control	5'-UGGGAGUCGGAAGAAGACUCGAUCA-3'
siRNA Lamin A/C	5'-UGGGAGAGGCUAAGAAGCAGCUUCA-3'

**Table.S4:** PCR Primers used

PCR primers	
Sun-1 -Forward	5'-CATGAAGTGCCTCTCTCCAA-3'
Sun-1 -Reverse	5'- CCTGCTTTCAGCTTGGTTTC-3'
Sun-2 -Forward	5'-CAGCAACATGAAGCACCTGT-3'
Sun-2 -Reverse	5'-GCTGCCGATGTAGGACTCTC-3'
Axin-2 -Forward	5'- TAGGCGGAATGAAGATGGAC-3'
Axin-2-Reverse	5'- CTGGTCACCCAACAAGGAGT-3'
18S -Forward	5'-GAACGTCTGCCCTATCAACT-3'
18S -Reverse	5'-CCAAGATCCAACACTACGAGCT-3'

**Table.S5:** Immunostaining antibodies and Reagents and their final concentrations

Immunostaining antibodies and Reagents	Final Concentration	
Nesprin-2 (IQ565).	Immunoquest	1/200
$\beta$ catenin (#610051)	Milipore	1/200
DyLight 649 Donkey Anti-Mouse	Immuno Research Laboratories	1/500
Alexa Flour 555 Donkey Anti-Rabbit	Invitrogen	1/500
Hoechst 33342	Invitrogen	1 $\mu$ g/mL
Alexa Fluor 488 Phalloidin	Life Technologies	0.1 $\mu$ M

**Table.S6:** Overexpression sequences and their final concentrations

Overexpression sequences	Final Concentration	
PEGFP-C1- $\beta$ catenin (#16071)	Addgene	1 $\mu$ g DNA per 100,000 cells

**Table.S7:** Overexpression and siRNA reagents and their final concentrations

Knockdown and overexpression Reagents	Final Concentration
---------------------------------------	---------------------

LipoD293 (overexpress)	SignaGen Laboratories	3 $\mu$ L per mL
PepMute Plus (siRNA)	SignaGen Laboratories	3 $\mu$ L per $\mu$ g of DNA
Puromycin (overexpress)	Sigma Aldrich	10 $\mu$ g/mL

### ***Isolation of Nucleoskeleton, soluble nuclear and nuclear envelope proteins***

Immediately following the mechanical challenge, cells were washed and pelleted in ice-cold PBS. Cell pellets were then resuspended in 0.33 M sucrose, 10 mM HEPES, pH 7.4, 1 mM MgCl<sub>2</sub> and 0.1% Triton X-100 (pellet vs. buffer, 1:5) then placed on ice for 15 minutes. After centrifugation at 3,000 rpm for 5 minutes, the supernatants were collected (cytoplasmic fraction) and same steps were repeated two more times to ensure highly enriched nucleus with minimal cytoplasmic contamination. Nuclear pellets were then resuspended in 0.45 M NaCl and 10mM HEPES, pH 7.4 and placed on ice for 15 minutes to rupture the nucleus and release soluble nuclear protein fraction. After centrifugation at 12,000 rpm for 5 minutes, the soluble nuclear fraction (it will be referred as nuclear fraction) will be collected. Remaining insoluble Lamin A/C rich pellet contains nuclear envelope, nucleoskeleton and chromatin (Fig.2)(Cook, 1988) This fraction was dissolved in 0.2% SDS for further analysis, this fraction will be referred as nucleoskeletal (Nsk) fraction. For the Nsk fraction, we have used LaminA/C as a referent. LaminA/C was compared to an alternative referent LaminB1. Our results showed no differences between laminB1 and LaminA/C (Fig.S6).

### **Co-localization Analysis**

MSCs were simultaneously immunostained against Nesprin-2,  $\beta$ catenin and DAPI and were imaged using Olympus IX-60 inverted microscope using a 40X magnification. Nesprin-2 was labeled via Nesprin-2 (IQ565) primary and Alexa Flour 555 Donkey Anti-Rabbit secondary

antibodies using indicated concentrations (**Fig. S5**). Nesprin-2 was visualized using Texas Red filter (Excitation 542-582, Emission 604-644).  $\beta$ catenin was labeled via  $\beta$ catenin (#610051) primary and DyLight 649 Donkey Anti-Mouse secondary antibodies using indicated concentrations (**Fig. S5**).  $\beta$ catenin was visualized using Cy5 filter ( Excitation 604-644, Emission 672-712). Image stacks were divided to individual channels and converted to 8-bit grayscale. Nuclear area of interest has been selected using DAPI stain as a mask where the region inside of the selected area was designated as “Intra-nuclear” and outside was designated as “Extra-nuclear”. Using the restore selection function, same areas of interests were extracted for Nesprin-2 and  $\beta$ catenin channels. Colocalization pixel map was generated using standard “colocalization threshold” option and average colocalization was plotted across the horizontal axis against nuclear position within a rectangular region of interest (Fig.3e and Fig.S1). Using nuclear position as a reference, extra-nuclear to intra-nuclear colocalization ratio was reported for each cell.

**Fig.S1- Co-depletion of LINC elements Sun-1 and Sun-2 displaces both Nesprin-2 and  $\beta$ catenin from nuclear envelope**

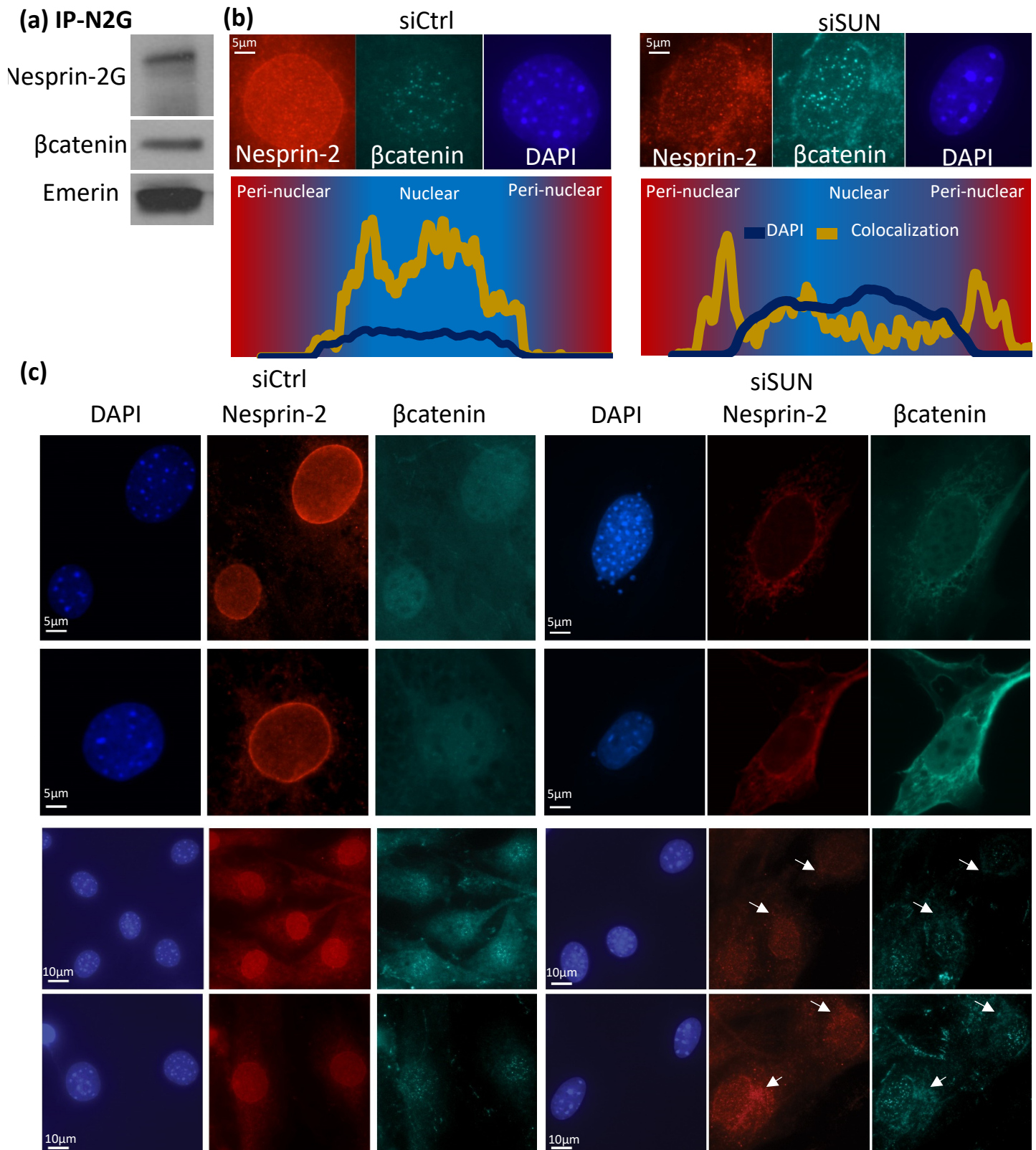


**Figure S1 a)** Immunoprecipitation of Nesprin-2 showed associations between  $\beta$ catenin and Emerin. **b)** Representative images of siCtrl and siSUN treated cells showing Nesprin-2 (red) and  $\beta$ catenin (green) distribution. In siCtrl treated cells, colocalization between Nesprin-2 and  $\beta$ catenin (represented as yellow line) remains intranuclear while in siSUN treated cells colocalization was shifted into perinuclear area and remains outside of the nuclear boundary (DAPI, blue line). Representative images of **c)** siCtrl and siSUN treated cells indicating the intracellular localization of Nesprin-2 (red) and  $\beta$ catenin (green) in relation to the nucleus (blue). White arrows indicate the perinuclear distribution of Nesprin-2 and  $\beta$ catenin in siSUN treated cells. .

**Fig.S2- Nuclear  $\beta$ catenin accumulation but not  $\beta$ catenin-nucleoskeleton association increase under sustained GSK3  $\beta$  inhibition**

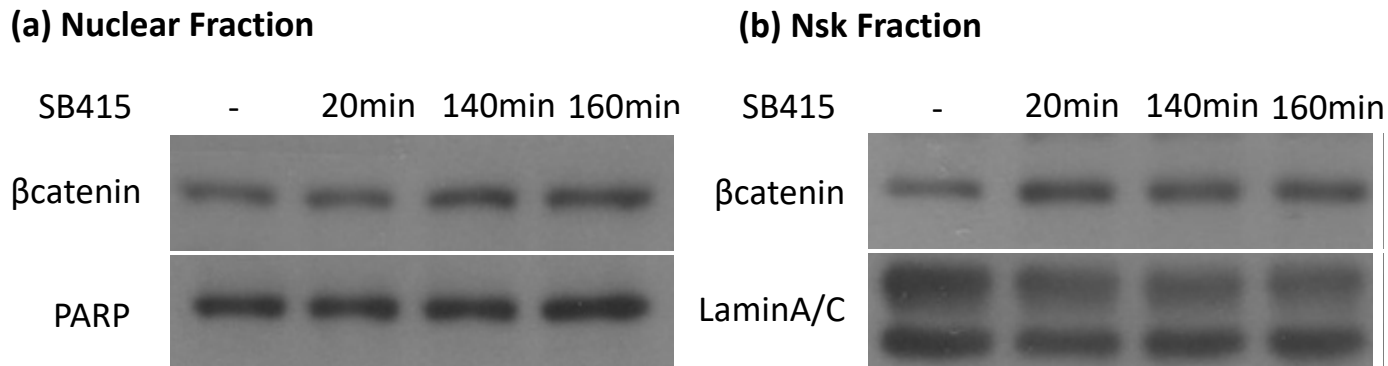
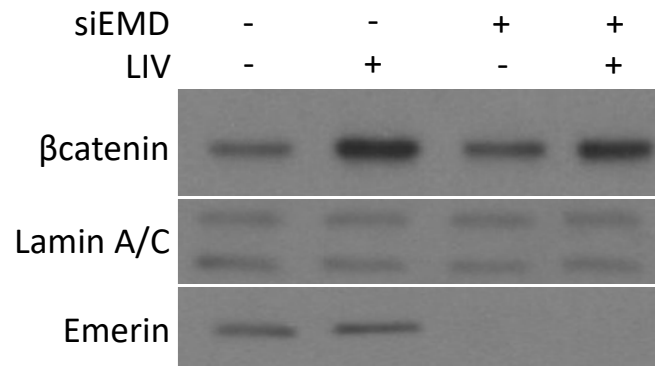


**Figure S2. a)** SB415 induced inhibition of GSK3 $\beta$  resulted in a stable increase of soluble nuclear  $\beta$ catenin at 20, 140 and 160 minute time points. **b)** SB415 induced inhibition of GSK3 $\beta$  resulted in an increased  $\beta$ catenin-Nsk association as soon as 20 minutes and upon keeping SB415 constraint,  $\beta$ catenin-Nsk association remained elevated at 140 and 160 minute time points but signal intensity was not changed.



**Fig.S3- Depletion of Emerin or LaminA/C are not sufficient to inhibit LIV-induced  $\beta$ catenin-nucleoskeleton association**

**(a) siRNA against Emerin (siEMD)**



**(b) siRNA against Lmna (siLmna)**

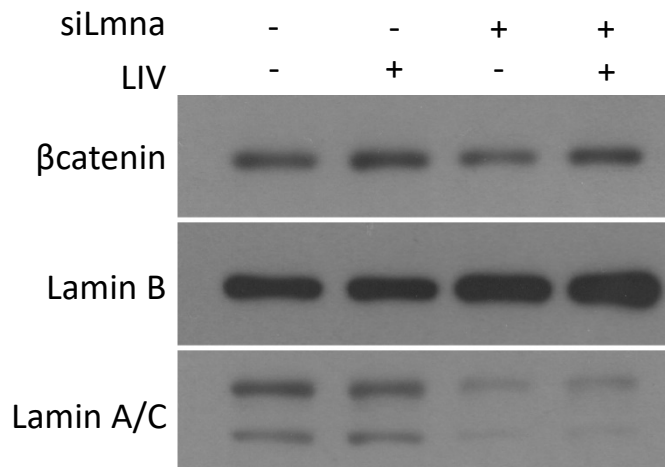


**Figure S3. a)** siRNA against Emerin (siEMD) did not change the basal and LIV-induced  $\beta$ catenin-Nsk association between siCtrl and siEMD MSCs. **b)** Similarly, siRNA against LaminA/C (siLmna) did not inhibit LIV-induced  $\beta$ catenin-Nsk association. LIV was applied at 90 Hz, 0.7g for 20 minutes. Samples were collected immediately after LIV application.

**Fig.S4- LINC elements Sun-1 and Sun-2 are necessary for strain-induced  $\beta$ catenin nuclear entry**

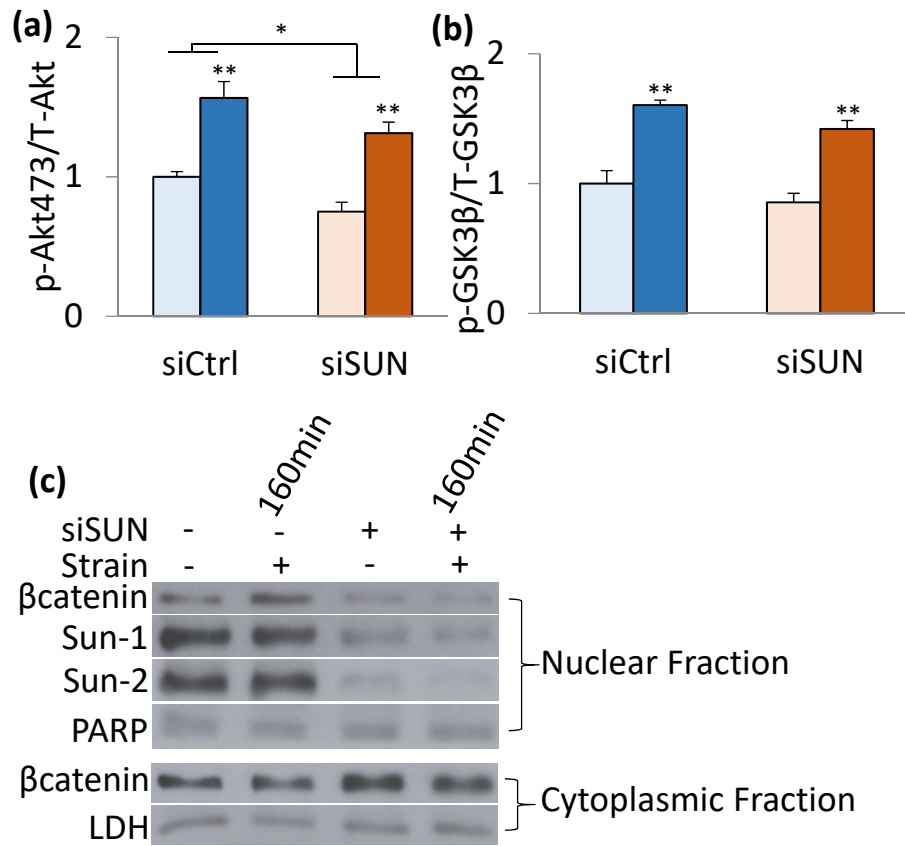


**Figure S4.** Application of strain results in **a)** Akt activation as well as **b)** GSK3 $\beta$  in both siCtrl and siSUN treated cells suggesting an increased  $\beta$ catenin pool in the cytoplasm (n=3). **c)** Separating soluble nuclear and cytoplasmic fractions 160 min post-strain showed that in siCtrl cells  $\beta$ catenin entered the nucleus while in siSUN cells there was no increase in nuclear  $\beta$ catenin and  $\beta$ catenin in the cytoplasmic fraction was increased. Group comparisons were made using One-way ANOVA followed by a Newman-Keuls post-hoc test (Fig.S4a-b). \* p<0.05, \*\* p<0.01, \*\*\* p<0.001, against control and each other.

**Fig.S5- Nesprin-2 Immunoprecipitation**

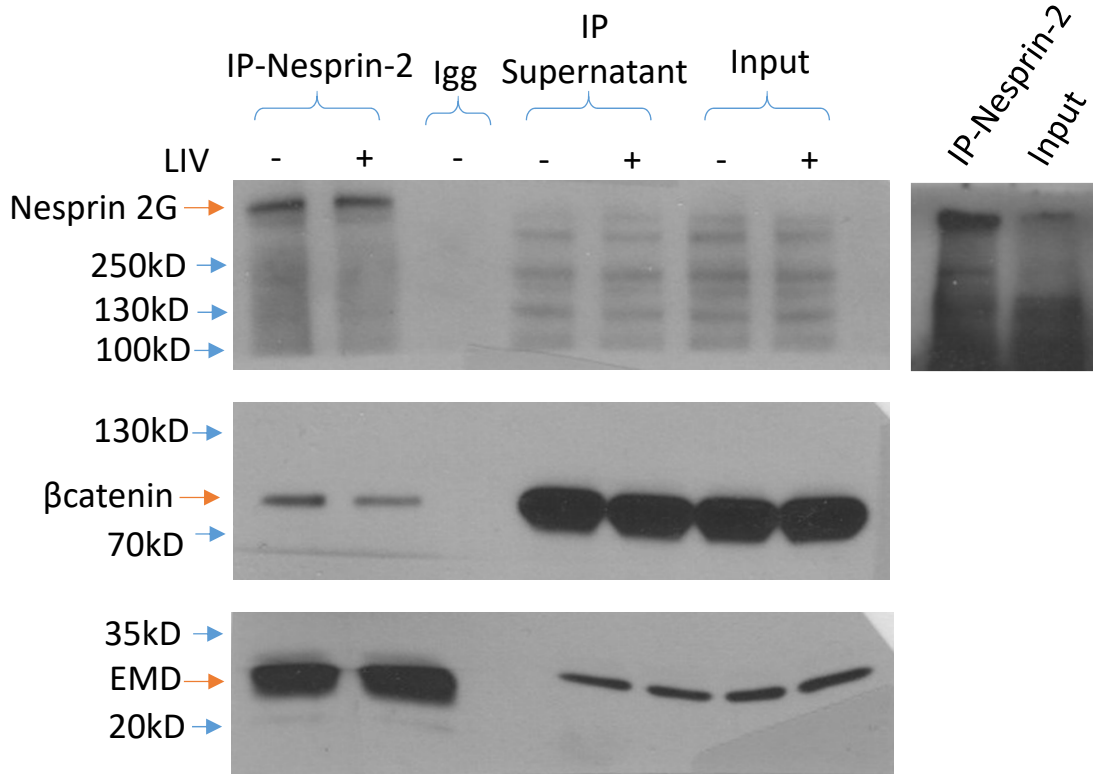


**Figure S5.** Supplementary file for Fig.4f displaying full size blots and other control lanes.

**Fig.S6- Comparison of LIV and strain induced changes of Lamin A/C and Lamin B1**

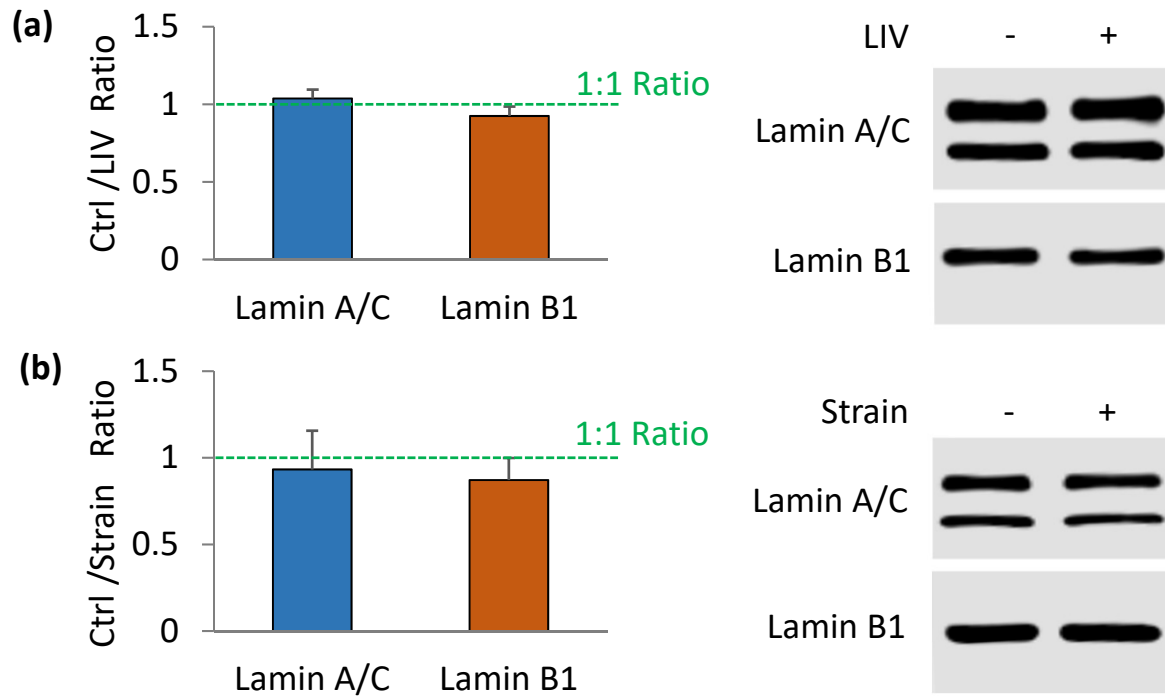


**Figure S6.** Changes in Lamin A/C and Lamin B1 protein amounts were reported as ratio between **a)** control and LIV samples (n=8) and **b)** control and strain samples (n=6). 120 minutes after the first mechanical challenge, no differences between LaminA/C and LaminB1 was detected in response to either LIV or Strain. Group comparisons were made using unpaired T-test (Figure S6a-b).

**Fig.S7- Total  $\beta$ catenin levels did not change with LIV**

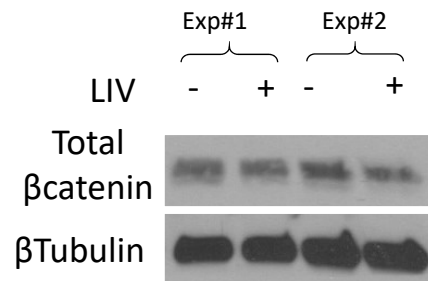


**Figure S7.** Whole cell lysates 160min post-LIV were probed via total  $\beta$ catenin(BD, 610154 ) and  $\beta$ -Tubulin (Santa Cruz, SC-9104)